J Appl Electrochem (2010) 40:2013–2022
DOI 10.1007/s10800-010-0181-z

ORIGINAL PAPER

Electrodeposition of Cu–Zn alloy coatings from citrate baths containing benzotriazole and cysteine as additives

F. L. G. Silva · D. C. B. do Lago · E. D'Elia · L. F. Senna

Received: 3 December 2009 / Accepted: 18 July 2010 / Published online: 5 August 2010

Abstract Alternative electrolytes, such as citrate baths, are now studied, aiming to reduce the toxicity and the cost of the electroplating process while maintaining the decorative qualities and anticorrosive properties of the coatings. For this purpose, brightening and/or leveling compounds are usually added to the base citrate bath. In this work, Cu–Zn alloys were electroplated on mild steel substrates from electrolytes containing sodium citrate and additives (benzotriazole and cysteine) at constant stirring speed. The results showed that coatings produced from baths containing additives were brighter than those obtained from the base citrate bath. Additionally, the presence of benzotriazole directly influenced the coating composition and the properties of the deposited alloy: the amount of zinc in this coating increased excessively, and the coating/substrate corrosion presented a poor anticorrosive performance.

Keywords Electrodeposition · Citrate bath · Additives · Cu–Zn alloys

F. L. G. Silva · D. C. B. do Lago · L. F. Senna (✉)
Departamento de Química Analítica, Universidade do Estado do Rio de Janeiro, Rua São Francisco Xavier, 524, Pavilhão Haroldo Lisboa da Cunha, Sala 427 – Maracanã, C.E.P. 20559-013 Rio de Janeiro, RJ, Brazil
e-mail: lsenna@uerj.br

E. D'Elia
Departamento de Química Inorgânica, Universidade Federal do Rio de Janeiro, Av. Athos da Silveira Ramos, no 149, Bloco A, Sala 634A, Ilha do Fundão, C.E.P. 21941-909 Rio de Janeiro, RJ, Brazil

1 Introduction

Electrodeposition is one of the most commonly used methods for metal and metallic alloy film preparation in many technological processes. Alloy metal coatings present a wider range of properties than those obtained by a single metallic film, and can be applied to improve the properties of a substrate/coating system. These coatings can be electrodeposited by the simultaneous reduction of two or more metallic cations present in an electrolyte solution. However, the simultaneous discharge of different ions on the cathode is not a simple process, and it can be influenced by the substrate surface, as well as by changes in the structure and activity of each metal cation in the double layer [1–4].

Simultaneous deposition is generally obtained by using complexant agents to decrease the activity of the nobler cation in solution [5–7]. Adherent Cu–Zn alloy coatings, with low porosity, are usually produced from alkaline cyanide baths, despite the high toxicity and the need for rigorous maintenance and control of the solutions [1, 8]. Moreover, the prolonged use of cyanide baths decreases the quality of the deposits produced. Several alternative and environmentally friendly electrolytes are now studied to produce Cu–Zn coatings with the same quality and properties shown by coatings obtained from cyanide baths [9–13]. Among the electrolytes studied in the literature, the citrate ions are well known as low molecular mass ligands, which form stable complexes with several trace metals in physiological media [14]. In fact, citrate-based electrolytes have been studied in the electrodeposition of copper [15], zinc [16], and their alloys [17]. Recently, it was possible to establish almost ideal conditions for the deposition of Cu–Zn alloys from citrate baths, producing coatings with compositions near that of commercial brass [18].

It is known that high quality, micrometer-thick films (smooth and bright deposits) can be prepared, at a reasonably high deposition rate, by using baths with a high concentration of metallic ions and small amounts of additives [19, 20]. Therefore, the properties of the deposits can be enhanced by using brightening and leveling substances, usually called additives, which can refine the grain size of the coating. Then, the morphological components of the layer are kept on the same plane, producing coatings that reproduce the original metal luster [3]. Since these substances can directly influence the deposition mechanisms of the alloy and the coating performance when exposed to an aggressive environment, each additive included in an electrodeposition bath must be carefully studied.

Benzotriazole (BTAH), a well-known corrosion inhibitor for copper, is one of the additives used for copper deposition from acidic baths [21], producing bright and level Cu coatings. It is assumed that BTAH addition can inhibit the surface diffusion of copper atoms in the beginning of the deposition process, decreasing the grain size of the coating. Amino acids are also applied as additives for the electroplating of copper and copper alloys, acting in the deposition process as surfactants adsorbed at copper surface, as copper ions complexants or even by decreasing the intensity of any parallel reaction [11, 22, 23]. Cysteine is one example of amino acid that can be applied as an additive for Cu–Zn deposition because it can adsorb on copper surface and, consequently, decrease significantly the cathodic current of the process by increasing the overpotential for hydrogen ion reduction [22, 23].

Earlier, it was demonstrated that sodium citrate can be used as a complexant for Cu–Zn coatings produced from electrodeposition baths [17, 18]. Since each alloy coating is a different system, and the use of different complexant agents and additives also contributes to several changes in the deposition processes [9, 24], it is fundamental to reach a better understanding of the electrochemical process and the effects of the deposition parameters on the coating properties before using it industrially. Therefore, in this work, the organic additives benzotriazole and cysteine were added to a citrate base electrolyte to verify the influence of these additives on the morphological and anticorrosive properties of Cu–Zn alloys on mild steel.

2 Experimental procedures

2.1 Cathodic polarization curves

Cathodic polarization curves were galvanostatically obtained in the current density range of 0.1–120 A m^{-2} using a potentiostat/galvanostat developed for this purpose [18]. AISI 1028 mild steel discs (with an exposed area of 1.70×10^{-4} m^2) were used as working electrodes. These samples were first polished with emery paper (100–600 mesh), washed with deionized water and alcohol and finally dried, before being immersed in the solutions described in Table 1. The counter electrode, was a very soluble 1.60×10^{-3} m^2 brass plate (63% m/m Cu, 37% m/m Zn), which generally dissolves with high efficiency and is usually used for Cu–Zn electrodeposition [25–27]. This electrode was immersed in a 10% v/v HNO_3/20% v/v H_2SO_4 solution for 1 min, immediately before being used in the experiments, to remove any oxide layer that could decrease its efficiency. This effect was also avoided by using excess of ligand during the experiment (Table 1). The reference electrode was a saturated mercury (I) sulfate electrode (Hg/Hg_2SO_4), SSE. Based on earlier results [18, 28], the experiments were carried out at room temperature with a stirring speed of 300 rpm.

2.2 Electrodeposition experiments

The electrodeposition experiments were carried out in triplicate series, using the same potentiostat/galvanostat and electrochemical cell described earlier. In these experiments, the working electrodes were AISI 1028 mild steel discs with an exposed area of 4.90×10^{-4} m^2. The cleaning procedures for both the work and the counter electrodes were the same described for the cathodic polarization curves (item 2.1). Based on the polarization curves and on earlier results [18, 28, 29], four current densities (10 A m^{-2}, 20 A m^{-2}, 30 A m^{-2} and 60 A m^{-2}) were selected to produce the Cu–Zn alloys on a steel substrate from the baths described in Table 1 at the same stirring speed (300 rpm). Each electrodeposition time was calculated, based on the Faday's law [30], to produce a 10 mg coating, and the cathodic current efficiency (E_f) was obtained gravimetrically. The produced layers were

Table 1 Chemical composition and the pH values of the baths studied

Bath no.	Composition/mol L^{-1}					pH
	$CuSO_4 \cdot 5H_2O$	$ZnSO_4 \cdot 7H_2O$	$Na_3C_5H_6O_7$	Benzotriazole	Cysteine	
1	0.02	0.20	1.00	–	–	6.59
2	0.02	0.20	1.00	0.001	–	6.52
3	0.02	0.20	1.00	–	0.001	6.77

dissolved in 20% v/v HNO_3, and the alloy composition was determined by flame atomic absorption spectrometry (FAAS), applying the conditions recommended by the instrument operation manual.

In order to verify if the amount of Cu^{2+} and Zn^{2+} ions were maintained for all the assays, the metal contents in the baths were always analyzed by atomic absorption spectrometry at the end of all the experiments performed with each bath. Moreover, the conductivity and pH of the baths were controlled, before and after each electrodeposition experiment.

Based on the electrodeposition experiments, galvanostatic transients were obtained. Partial polarization curves were also plotted by calculating the effective corresponding currents for copper and zinc deposition from the element contents in the alloy coating and the current efficiency [2]. In each case, the partial currents were associated with the corresponding potential response of the total applied current density.

2.3 Morphological analysis

Scanning electron microscopy (SEM) was performed using a *JEOL JSM 6460LD* microscope to evaluate the effect of the deposition parameters on the surface morphology of the coatings produced.

2.4 Corrosion experiments

Based on the chemical and morphological analyses, Cu–Zn coatings were produced on steel substrate from the electrolytes presented in Table 1 at 30 A m^{-2}, employing a potentiostat/galvanostat PG29 (*Ominimetra Instruments*). The experiments were performed in a 0.5 mol L^{-1} NaCl solution (pH = 6.5) at room temperature. The counter electrode was a platinum net, while the reference electrode was a saturated calomel electrode (SCE).

3 Results and discussion

3.1 Cathodic polarization curves

The polarization curves of the steel electrode, obtained from the solutions described in Table 1 at 300 rpm, are presented in Fig. 1. These experiments aimed to select the current density values to obtain alloy deposits. Earlier experiments [18, 28, 29] have shown that a decrease in the current density favors the copper deposition. Breder et al. [28] have also shown that the amount of copper deposited at current densities smaller than 10 A m^{-2} were 100%, mainly in Baths 1 and 3. After analyzing the curves in Fig. 1, and based on these earlier results, four current

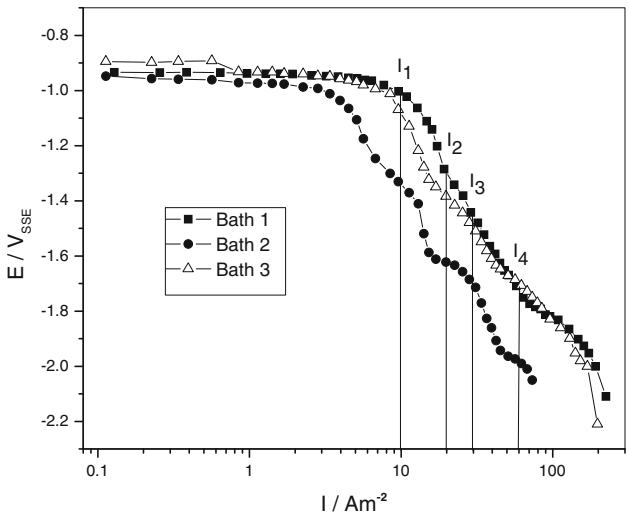

Fig. 1 Polarization curves of the steel electrode, obtained from the solutions described in Table 1 at 300 rpm

densities (10 A m^{-2}, 20 A m^{-2}, 30 A m^{-2} and 60 A m^{-2}) were chosen for the electrodeposition experiments. Since it was intended to produce Cu–Zn alloys and compare the coatings produced from the three baths at the same conditions, we have chosen the current density values beginning at 10 A m^{-2} and continuing until 60 A m^{-2} (approximately −1.80 V_{SSE}), where HER should predominate compared to zinc reduction.

These curves can also show the effects of the organic additives on the cathodic behavior of the substrate. For all solutions, the polarization curves have different slopes in different current density ranges, which are probably associated with several deposition mechanisms [31]. Comparing the three polarization curves, there is a substrate polarization for the samples immersed in Bath 2, where benzotriazole is present. Earlier works, dealing with Copper-alloys electrodeposition with citrate baths, containing or not additives [15, 18, 28, 29] have shown that both the ligand and the Cu–citrate complexes can adsorb on the cathode surface, causing a substrate polarization. This effect decreased with the increasing of solution stirring. In the present work, the substrate polarization observed in Bath 2 could not be related to the blocking citrate effect, since citrate was the main ligand for all three baths. Moreover, all experiments were carried out in stirred solutions, which must have compensated the adsorption (blocking) effect. Therefore, it is probably to suppose that, in this work, the substrate polarization observed for this bath could be related to the presence of benzotriazole in it. Benzotriazole is well known as an excellent corrosion inhibitor for copper and its alloys due to the formation of a Cu(I)-BTAH polymeric protective film on the metal surface [21]. This film can be adsorbed on the substrate surface, acting as a blocking species and causing the observed

polarization. On the other hand, no significant changes were observed when cysteine was added to the citrate bath (Bath 3). This additive acts as a corrosion inhibitor for copper by working in the cathodic part of the Tafel curve, increasing the hydrogen overpotential [23]. Since the hydrogen evolution reaction (HER) can compete with zinc reduction at higher current densities, the presence of cysteine could enhance zinc deposition, showing a substrate depolarization in the polarization curves. This effect, however, was not observed in Fig. 1.

3.2 Electrodeposition experiments

The electrodeposition of Cu–Zn alloys from the baths presented in Table 1 was performed for the selected current densities at 300 rpm. Figure 2 presents the cathodic current efficiency (CCE) values for the alloy electrodeposition. The CCE values for the coatings obtained from Baths 1 and 3 were always above 80%, no matter the current density applied. In contrast, the CCE values for the alloys produced from Bath 2 were always lower than 70% for all conditions studied. Moreover, a significant increase ($p < 0.002$) of CCE values with the applied current density was also observed for the coatings produced from this bath. The substrate polarization observed in Fig. 1 can be related with the results verified in Fig. 2. In the presence of BTAH, the copper reduction becomes more difficult due to a blocking compound on the substrate surface (the polymeric Cu(I)–BTA complex, for example [21]), which favors other parallel reactions, such as the HER from the water. In fact, lower CCE values found at low current densities suggest that H_2 evolution may be favored in this condition. However, when the potential for zinc reduction was reached, at higher cathodic polarization, the deposit was probably enriched with this metal, increasing the CCE.

Figure 3 presents the copper and zinc content in the coating for layers produced from the baths described in Table 1. It is possible to observe the contrasting behavior of copper (Fig. 3a) and zinc (Fig. 3b) amounts with the applied current density for Baths 1 and 3: increasing the applied current density causes a decrease in the copper content and an increase in the zinc content. These results are similar to those reported by Ferreira et al. [18]. Since Cu is the noblest metal in the solution, its ions are usually easily reduced, and this is probably the main reaction observed, mainly at low values of current density. However, the increase of this deposition parameter causes other parallel reactions, such as Zn reduction and/or HER, decreasing the amount of copper in the coating. Therefore, large current densities are needed to promote a significant

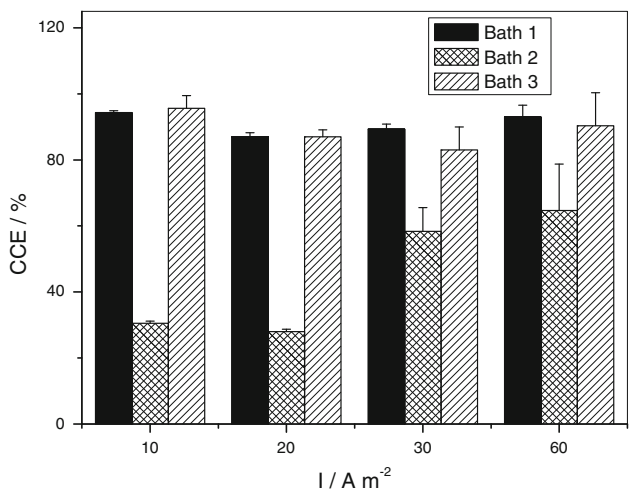

Fig. 2 Cathodic current efficiency (CCE) of the coatings produced with the solutions described in Table 1 at 300 rpm

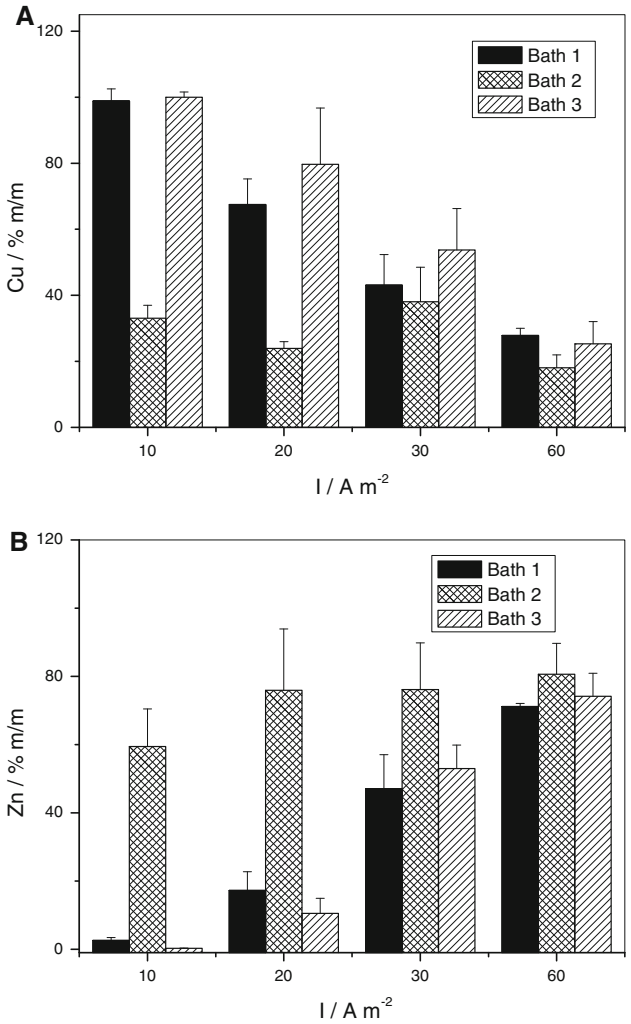

Fig. 3 **a** Copper and **b** Zinc contents in the coatings produced with the solutions described in Table 1 at 300 rpm

reduction of zinc ions to metallic zinc on the substrate using these baths.

The deposition process for coatings produced from Baths 1 and 3 changes from regular (that is, Cu content > Zn content in the coating) to anomalous (Zn content > Cu content in the coating [32]) with the applied current density. At 30 Am^{-2}, the amounts of Cu and Zn in the deposits are approximately the same (43% m/m Cu and 47% m/m Zn for Bath 1, and 54% m/m Cu and 53% m/m Zn, for Bath 3). Moreover, the amount of copper in coatings produced from Bath 3 is higher than the values obtained for those deposited from Bath 1 for most of the current densities studied (Fig. 3a). The presence of cysteine in citrate baths can possibly favor the copper deposition compared to the base citrate bath (Bath 1). Senna et al. [9] have shown that the presence of saccharine in pyrophosphate Cu–Zn baths provoked an increase in copper content in the coating. The authors suggested that this additive could have decreased the stability of the Cu–pyrophosphate complex, promoting copper deposition. Therefore, the same process may occur with Cu–citrate complexes.

It is also important to point out that, while the coatings produced from Bath 1 at the highest current densities (60 A m^{-2}) presented a dull grayish color and low adhesivity, those obtained from Bath 3 under the same conditions were bright and reddish. Since HER is enhanced at high current density values, the consequent increase in pH values near the electrode surface may occur [9, 18]. In solutions containing only Zn–citrate complexes in the pH range between 6.0 and 7.0, Gusev et al. [16] also suggested that the cathode could become passivated by hydroxides due to the decomposition of complexes. As these complexes undergo discharge, the layer next to the electrode becomes alkaline because of hydrolysis of the released citrate ions according to the reaction $C_6H_4O_7^{4-} + H_2O \Leftrightarrow C_6H_4O_7^{3-} + OH^-$, which also contributes to the appearance of hydroxyl ions in the layer next to the electrode. This effect was probably minimized in citrate baths containing cysteine, and the coatings produced at 60 A m^2 still presented good appearance. The increase in hydrogen overpotential [23], caused by the presence of cysteine in the bath (Bath 3), may have prevented direct zinc incorporation as zinc hydroxide and probably stimulated the zinc electroplating (Fig. 3b).

On the other hand, the deposition process of Cu–Zn coatings from Bath 2 was always anomalous, no matter the current density used. The deposits were bright, and their colors varied from yellow to yellow-grayish as the current density increased, in agreement with the increase in zinc content in the coating, both in metallic and hydroxide forms (Fig. 3b). It is also possible to compare these results with the polarization curves (Fig. 1), where the strong polarization can be associated with a blocking species on the substrate surface (perhaps the polymeric Cu(I)–BTA complex). Moreover, the diffusion of free cuprous ions on the cathode surface may become less favorable in the presence of BTAH, and the reduction of cuprous ions takes place primarily through the Cu(I)–BTA complexes [21]. These features may be responsible for the low copper content (below 40% m/m) in the coatings produced from this bath.

The potential variation with time was measured for each deposition process. Figure 4 presents the galvanostatic transients for the deposition process at two current density values (10 A m^{-2} and 60 A m^{-2}). In Fig. 4a (10 A m^{-2}), a potential decrease was observed immediately after the chosen current density value was applied, which can be associated with a nucleation process. This process was

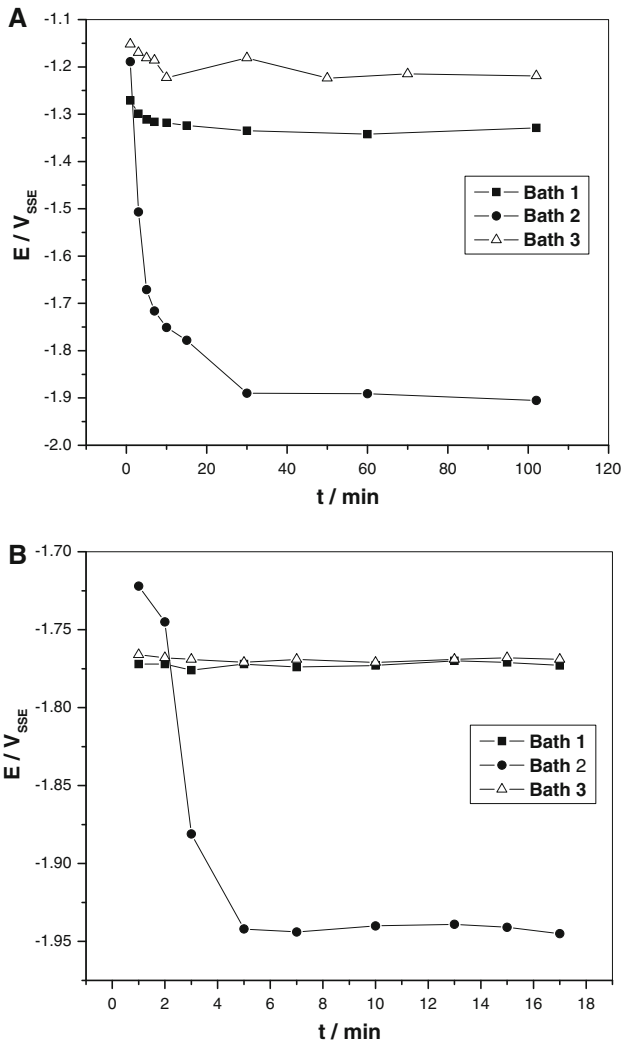

Fig. 4 Examples of galvanostatic transients obtained during the electrodeposition experiments with the solutions described in Table 1 at 300 rpm: **a** 10 A m^{-2}; **b** 60 Am^{-2}

more intense for the coating produced from Bath 2. As the experiment continues, the potential reaches a stable value, corresponding to a grain growth stage. Similar results were observed for Bath 2 in Fig. 4b (60 A m^{-2}), although the initial potential decrease could not be noted for Baths 1 and 3. As the applied current density increased, the stabilized potential range was more negative for all baths.

The polarization observed for Bath 2 in Fig. 4a and b can be related to a decrease in the surface diffusion of copper ad-atoms [21]. A small surface diffusion can enhance the nucleation process, resulting in a sharp variation of potential with time, as noted for Bath 2. This may also indicate the presence of small islands of copper deposits on the substrate surface. In addition, after the deposition proceeded for a finite time, a limit current was reached (Fig. 1) due to copper ions depletion on the cathode surface and the fact that the mass transport was insufficient to replenish the metal ions. Leung et al. [21] showed, for copper sulfate acid baths, that BTAH adsorbs on the surface of the islands and passivates the deposition process. These islands then stop growing. However, due to the galvanostatic mode of operation, deposition continues by nucleation of other islands, and a random deposition takes place, in which the nucleation rate is almost four times higher than that of the bath without this additive [33]. The presence of this additive may also decrease the size of the islands. It is then expected that coatings produced from Bath 2 will present small grain sizes. On the other hand, the citrate-base bath (Bath 1) and that one containing cysteine (Bath 3) did not presented this behavior, which probably indicates that the grain growth is favored in deposits produced from these baths, and that their coatings may present higher grain sizes than those produced by Bath 2. Furthermore, there is a depolarization of the galvanostatic transient curve for the coatings produced from Bath 3, mainly at low current density values (Fig. 4a), which can correspond to the high amounts of copper in the coatings when compared to the coatings produced from Baths 1 and 2 (Fig. 3a). This depolarization was not observed in the polarization curves of Fig. 1, showing the limitation of this technique to describe the dependence of the cathodic process on the deposition electrolyte composition. Although cysteine can be a binder for Cu^{2+} ions in aqueous media due to the thiol and carboxylate groups, Cu(II)–thiolate complexes are generally unstable. It is often assumed that Cu^{2+} may enter in a redox couple with thiols of two cysteine molecules, in which Cu^{2+} is reduced to Cu^{+} and the thiol is oxidized to a disulfide [34, 35], resulting in a Cu(I)–cystine (two oxidized cysteine molecules, connected by a disulfide bond) complex, where Cu(I) is bound to two amino groups and two carboxylate groups [35]. Then, if cysteine also adsorbs on the substrate surface and, similar to what has been seen for BTAH, the Cu^{2+} ions reduction take place through the Cu(II)–cysteine complexes, the instability of these complexes, added to stable Zn(II)–cysteine complexes [36], may favor copper deposition, resulting in a higher copper content in the deposit. However, to the best of our knowledge, there is no work correlating any Cu–cysteine or Zn–cysteine complexes to copper or brass deposition. Therefore, a more detailed investigation needs to be carried out in order to fully support these hypotheses.

The partial polarization curves (Fig. 5) show the mass contribution of each alloy element and their corresponding current efficiencies in the alloy formation, as well as the effect of additives, during the complex electrodeposition process of a metallic alloy. The HER curve was calculated by the difference between the total applied and the metallic (copper + zinc) current densities. The copper partial polarization curves for Bath 1 in Table 1 (Fig. 5a) is near the total curve, mainly at small current density values, indicating that the alloy produced in these conditions is rich in copper. Then, the copper curve presents a polarization showing that copper deposition was less favourable at high values of current density, in agreement with Fig. 3a. On the other hand, the zinc partial current density increases linearly, crossing the copper curve for a total applied current density value of 30 A m^{-2} (where the zinc and copper contents are approximately the same, as shown in Fig. 3), and reaches close to the total curve at 60 Am^{-2}, confirming the anomalous deposition process in this condition. The HER curve shows a linear increase with the applied current density until 20 Am^{-2}. At this point, the potential value seems to be more favourable to zinc deposition, and the HER curve becomes polarized. It is important to point out that this effect can probably be related to the pH increase at the interface substrate/electrolyte, causing zinc deposition as zinc hydroxides. Since the partial polarization curves take into account the content of the deposited metal, and the HER curve was calculated based on these values, the HER curve might have been masked by these effects, and a polarized curve was observed.

The potential values observed for the alloy deposition from Bath 2 (Fig. 5b) are more negative than those verified for the coatings produced from Bath 1 under the same conditions (Fig. 5a). Compared to Fig. 5a, the copper partial curve for Bath 2 is distant from the total polarization curve, while the zinc one is near the total curve, confirming the anomalous deposition process observed for this bath. At low current density values, the summation of copper and zinc partial current densities is always smaller than the applied current density value. Moraes et al. [37] have shown that the contribution of the HER to copper electrodeposition process in acid medium was more significant in the presence of BTAH. In fact, the HER curve is near the total curve, showing its contribution to the process.

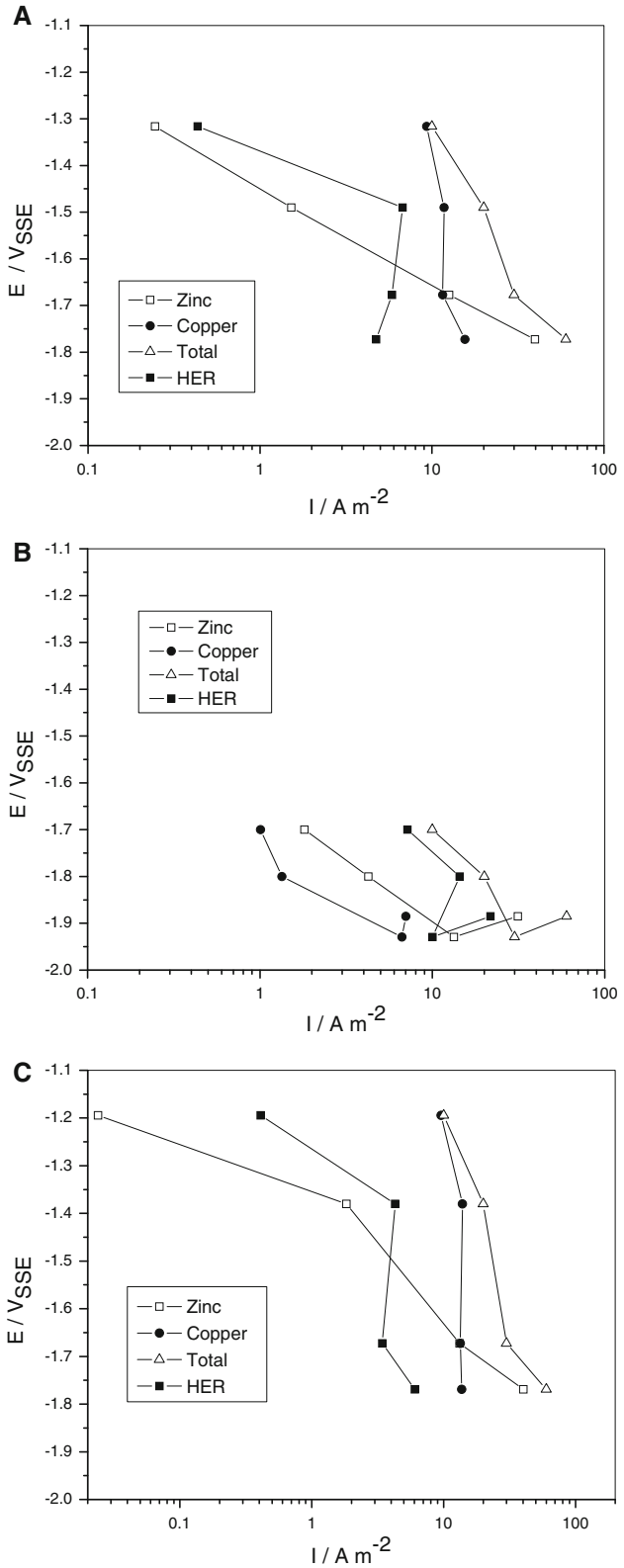

Fig. 5 Partial polarization curves of alloy electrodeposition from the baths described in Table 1 at 300 rpm: **a** Bath 1; **b** Bath 2; **c** Bath 3

However, in the present work, the pH value was 6.52 (Table 1). Therefore, the HER must occur mainly from the water hydrogen reduction, consuming part of the applied current density. On the other hand, at high values of current density, the zinc reduction must compete with the HER for the applied current. A small depolarization was observed at 60 A m^{-2}, probably related to changes on the deposition surface during the process [38].

Figure 5c shows the partial polarization curves for the alloy deposition from Bath 3. It is possible to note that, at applied current density value of 10 A m^{-2}, the alloy was deposited at less negative potentials compared to Baths 1 and 2 (Fig. 5a, b, respectively), which is in agreement with the galvanostatic transients observed in Fig. 4a. At this current density value, the copper and the total polarization curves are the same, while the zinc partial current density was far from the total curve, showing that its contribution to the process was negligible. Increasing the applied current density caused a polarization in the copper partial curve, and the copper and zinc curves cross over for the deposits produced at an applied current density value of 30 A m^{-2}. After this point, the change to the anomalous deposition process can be observed. As expected, HER curve is more polarized than those verified for Baths 1 and 2. Cysteine increases the overpotential for HER, decreasing the current density consumed by this parallel reaction. Compared to Bath 1, the current density values for zinc are always higher, except for 10 A m^{-2}, showing that this additive could be use to enhance the zinc deposition. However, Gockel et al. [36] have shown that stable zinc–cysteine complexes can be formed, and this fact might contribute to the small values noted in the partial current densities for zinc. In fact, the copper current densities were also higher than those found for Bath 1, except at 60 A m^{-2}. This can also be correlated to a probable interference of this additive in the stability of copper–citrate complexes.

It is important to point out that both the conductivity and pH of the baths have not changed significantly as the experiments proceeded. In fact, no precipitation or significant composition changes were observed, even at conditions where the anodic efficiency was probably higher than the cathodic one (Bath 2). Moreover, the chemical analysis of each bath at the end of the experiments have showed that the copper concentration did not changed (in all solutions), and the zinc concentration decreased by only 0.02 concentration unity, only in Bath 2, where the amount of copper deposited was always smaller than the zinc one. These results guaranteed that the metal contents in all baths remained practically constant during all the experiments.

3.3 Electrochemical and morphological experiments

Figure 6 shows the electrochemical results for Cu–Zn layers produced from the baths described in Table 1, at 300 rpm and 30 Am^{-2}, and compares their electrochemical behaviors with samples of copper, zinc and commercial brass (70% m/m Cu and 30% m/m Zn). In addition, Fig. 7 presents the surface micrographs of the coatings produced under the same conditions used for the electrochemical experiments (Fig. 6).

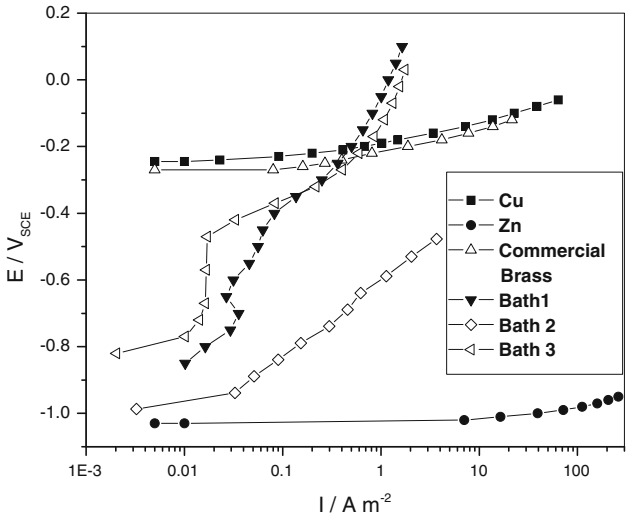

Fig. 6 Anodic polarization curves of commercial brass, copper, zinc, and the coatings produced from the solutions of Table 1 at 300 rpm and 30 A m^{-2}. Electrolyte: NaCl 0.5 mol L^{-1}, pH = 6.5, 25 °C

The coatings presented electrochemical performances between those of pure copper and pure zinc, which was expected for brass coatings, although their behaviors were very different from that of commercial brass. However, it is important to point out that most of the electrolytically-obtained alloys, produced from different baths, usually consist of fine crystals, non-uniform in composition and characterized by a considerable distortion of the crystal lattice, originating from the formation of the non-equilibrium phases at the cathode [3]. Lattice distortion can be responsible for non-homogeneous microscopic residual stress and can significantly contribute to the coating microhardness [24, 39]. Therefore, although adherent coatings were produced, several microdefects could probably exist on the coating surface, permitting the attack of the substrate by the aggressive medium and contributing to the different behaviors observed for the coatings and the commercial brass.

Comparing the coating performance in the electrolytic media (0.5 mol L^{-1} NaCl solution), it is interesting to note different behaviors between the substrate/coatings systems obtained from Baths 1 and 3, and those produced from Bath 2 (Fig. 6). This can be explained by comparing the results shown in Fig. 3 and the micrographs observed in Fig. 7. The copper and zinc contents of the coatings produced from Baths 1 and 3 are very similar, while coatings produced from Bath 2 presented higher zinc content (Fig. 3). This agrees with their respective corrosion potential values (−0.850 V_{SCE}, −0.939 V_{SCE}, and −0.820 V_{SCE}, for coatings from Baths 1, 2 and 3, respectively), and with the

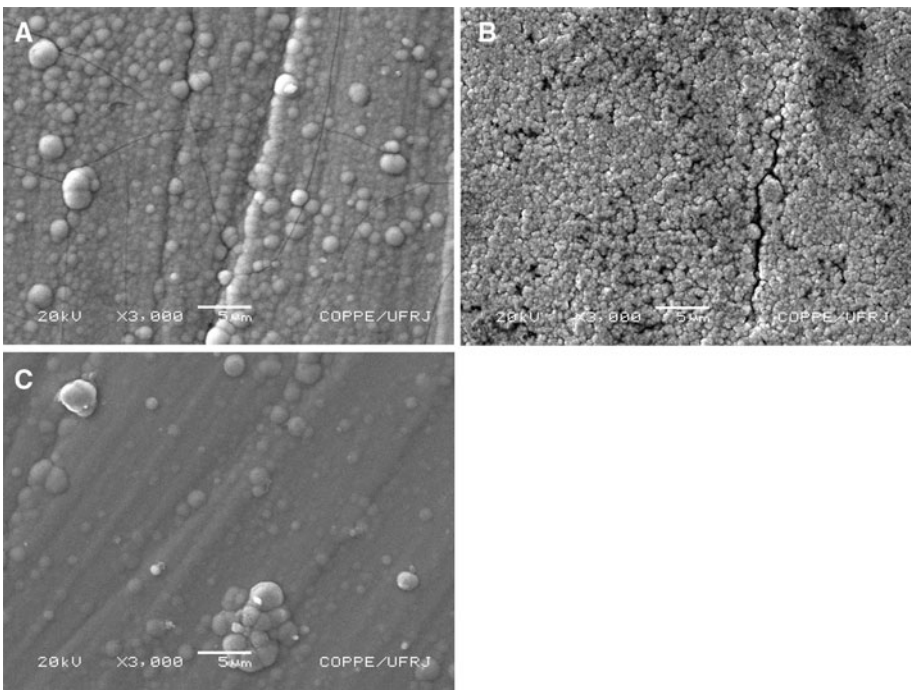

Fig. 7 Morphology of the coatings produced with the solutions of Table 1 at 300 rpm and 30 A m^{-2}: **a** Bath 1; **b** Bath 2; **c** Bath 3

higher values of anodic currents observed from the coatings produced from Bath 2. This coating curve presents anodic behavior closer to that of pure zinc than the others, corroborating the high zinc content in the deposits obtained from Bath 2, as shown in Fig. 3. It can be noted that, while the coatings produced from Bath 1, without additives, present coarse grains, with cracks and agglomerates (Fig. 7a), the coatings from the baths containing additives show a decrease in the grain size (Fig. 7b, c), which probably indicates that, under the conditions of these experiments, the nucleation rates of copper and zinc crystallites increase faster than the growth rate, mainly for coatings produced from Bath 2 (Fig. 7b), as shown earlier in Fig. 4. Although the coatings obtained from Bath 2 presented a smaller grain size than those shown in Fig. 7a, they also show several pores and cracks, which can facilitate the corrosion attack of the substrate. Moraes et al. [37] have already demonstrated that the addition of BTAH to a bath for copper deposition produced less crystalline coatings when compared with a bath free of this additive. However, after the corrosion experiment, this coating (which presented a gray-yellowish color) turned yellow. It indicates that the surface coating shown in Fig. 7b was probably a non-adherent coating, formed by zinc direct deposition as zinc hydroxides and/or hydrated zinc oxides, due to a local pH increase caused by the water reduction. Similar behavior has been observed in the literature [9, 39, 40].

On the other hand, the coatings produced from Bath 3 showed the smallest anodic currents for the same potential range. Additionally, no significant variation could be observed for the coating surfaces, which presented a red-yellowish color before the experiments. This result can possibly confirm the effect of cysteine in decreasing the HER and preventing the local pH increase. The coatings produced from Bath 3 presented small grains, several agglomerates (Fig. 7c) and a higher copper content (Fig. 3). Moreover, the zinc–cysteine complex can also contribute to preventing zinc direct deposition. It is also important to point out, however, that the presence of cracks may have affected the electrochemical performance of the coatings from Bath 1, when compared with those from Bath 3.

4 Conclusions

The addition of both benzotriazole (BTAH) and cysteine (Cys) as additives to the base citrate bath (Bath 1) affected the electrochemical process in the production of Cu–Zn alloy coatings on mild steel substrates. A strong substrate polarization was observed for Bath 2 (containing BTAH), possibly due to the Cu(I)-BTAH film formation on the substrate. This way, the coatings produced from this baths presented an anomalous deposition process for all current density values studied. Moreover, an abrupt potential decrease with time was also observed for coatings obtained from Bath 2, which was in agreement with the small size grains observed for these layers. These coatings presented several pores and a poor anticorrosive performance, probably due to a direct zinc deposition as zinc hydroxide and/or zinc oxides.

On the other hand, the coatings produced from Bath 3 were bright, even at elevated current density values, and presented higher copper contents than coatings obtained from Bath 1. The presence of Cys in the electrodeposition bath increases the potential for HER, and, at the same time, seems to prevent zinc direct deposition. These coatings presented the best anticorrosion performance among the coating/substrate systems tested in this work.

Acknowledgments The authors would like to thank the Rio de Janeiro Research Foundation (FAPERJ), the Brazilian National Research Council (CNPq), and the State University of Rio de Janeiro (UERJ) for financial support and Antônio Vitor de Castro for technical support. We would also like to thank the deceased student Helen Breder for the performance of some of the experiments presented in this paper.

References

1. Díaz SL (1988) Eletrodeposição de Ligas Cu/Zn. COPPETEC Projeto no. PP-3414. Universidade Federal do Rio de Janeiro, Rio de Janeiro
2. Senna LF (1991) Estudo de Parâmetros para Eletrodeposição de Ligas Cu/Zn em Eletrólitos de Pirofosfato. M.Sc. Dissertation, Universidade Federal do Rio de Janeiro, Rio de Janeiro
3. Vagramyan TA (1970) In: Kruglikov SS (ed) Electrochemistry. Israel Program of Scientific Translation Ltd., Jerusalem
4. Lainer VI (1970) Modern electroplating. Israel Program of Scientific Translation Ltd., Jerusalem
5. Fujiwara Y, Enomoto H (2000) J Electrochem Soc 147:1840
6. Fujiwara Y, Enomoto H (1988) Surf Coat Techn 35:101
7. Gómez E, Llorente A, Alcobe X et al (2004) J Solid State Electrochem 8:82
8. Zoppas J (1982) Contribuição ao Estudo da Influência do Cianeto em Soluções Alcalinas para Eletrodeposição de Zinco. M.Sc. Dissertation, Universidade Federal do Rio Grande do Sul, Porto Alegre
9. Senna LF, Díaz SL, Sathler L (2003) J Appl Electrochem 33(12):1155
10. Krishnan RM, Muralidharan VS, Natarajan SR (1996) Bull Electrochem 12(5–6):274
11. Mohamed AE, Rashwan SM, Abdel-Wahaab SM et al (2003) J Appl Electrochem 33(11):1085
12. Antón RL, Fdez-Gubieda ML, García-Arribas A et al (2002) Mater Sci Eng A 335:94
13. Johansen KD, Page D, Roy S (2000) Electochim Acta 45:3691
14. Kotsakis NC, Raptopoulou P, Tangoulis V et al (2003) Inorg Chem 42(1):22
15. Chaissang E, Quang KV, Wiart R (1986) J Appl Electrochem 16:591
16. Gusev VN, Bezzubov AL, Kochman ED (1977) Sov Electrochem 13(1):111
17. Ferreira FBA, Afonso PKC, Luna AS et al (2005) Electrodeposition of Cu-Zn alloys from alternative electrolytes. In:

Proceedings of the 2nd Mercosur congress on chemical engineering, Rio de Janeiro
18. Ferreira FBA, Silva FLG, Luna AS et al (2007) J Appl Electrochem 37:473
19. de Leon PFJ, Albano E, Salvarezza VRC (2002) Phys Rev E 66:1
20. Schlesinger M, Paunovic M (eds) (2000) Modern electroplating. John Wiley, New York
21. Leung TYB, Kang M, Corry BF et al (2000) J Electrochem Soc 147(9):3326
22. Marti EM, Methivier Ch, Pradier CM (2004) Langmuir 20:10223
23. Matos B, Pereira LP, Agostinho SML et al (2004) J Electroanal Chem 570:91
24. Senna LF, Díaz SL, Sathler L (2005) Mater Res 8(3):275
25. Durney LJ (1984) Electroplating engineering handbook. Springer, New York
26. Cobley AJ, Grabe DR (2002) Trans Inst Metal Finish 80:B13
27. Tremmel RA (1985) Cyanide-free copper electrolyte and process. United State Patent, no. 4,521,285, Michigan
28. Breder H, Lago DCB, Senna LF et al (2006) Efeito de aditivos nas propriedades anticorrosivas de revestimentos de liga Cu/Zn. In: Proceedings of the 2nd corrosion Latino American congress, Fortaleza
29. Silva FLG, Garcia JR, Cruz VGM et al (2008) J Appl Electrochem 38:1763
30. Christian GD, O'Reilly JE (1986) Instrumental analysis, 2nd edn. Allyn and Bacon, Inc., London
31. Greef R, Peat R, Peter LM et al (1985) Instrumental methods in electrochemistry. Ellis Horwood Ltd., London
32. Brenner A (1963) Electrodeposition of alloys V. 1 and 2. Academic Press, New York
33. Kim JJ, Kim SK, Bae JUk (2002) Thin Solid Films 415:101
34. Johnson AM, Holcombe JA (2005) Anal Chem 77:30
35. Dokken KM, Parsons JG, McClure J et al (2009) Inorg Chim Acta 362:395
36. Gockel P, Vahrenkamp H, Zuberbühler AD (1973) Helv Chim Acta 76:511
37. Moraes ACM, Siqueira JLP, Barbosa LL et al (2009) J Appl Electrochem 39(3):369
38. Paunovic M, Schlesinger M (2006) Electrochemical deposition, 2nd edn. John Wiley & Sons. Inc, New Jersey
39. Senna LF, Achete CA, Hirsch T et al (2005) Surf Eng 21(2):144
40. Ishikawa M, Enomoto H, Matsuoka M et al (1994) Electrochim Acta 39(14):2153